



Learning Amyloid Pathology Progression from Longitudinal PiB-PET images in Preclinical Alzheimer's disease

International Symposium on Biomedical Imaging, 2020

Wei Hao [1] Nicholas M. Vogt [1] Zihang Meng[1] Seong Jae Hwang [2] Rebecca L. Koscik [1]
Sterling C. Johnson [1,3] Barbara B. Bendlin [1] Vikas Singh [1]

[1] University of Wisconsin-Madison [2] University of Pittsburgh [3]William S. Middleton
Memorial Veterans Hospital



Hi! I am Wei Hao, an undergrad student
from U of Wisconsin- Madison,

Today, I'll talk about [Title]. This is a joint
work with Nicholas Vogt , Zihang Meng,
Seong Jae Hwang, Rebecca Koscik, Sterling
Johnson, Barbara Bendlin and Vikas Singh.

NEUROIMAGING AND ALZHEIMER'S DISEASE (AD)

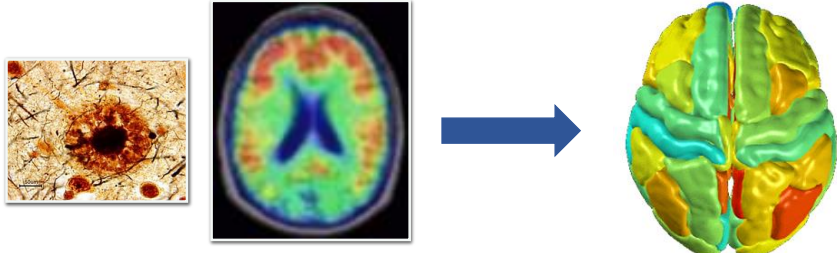
- Alzheimer's disease (AD)
 - Neurodegenerative disease
 - One of the leading causes of dementia
- Neuroimaging data
 - Measures specific pathologies related to AD



First, I want to provide a little bit of background information.

Alzheimer's disease, is a neurodegenerative disease, one of the leading causes of dementia. One way to understand Alzheimer's disease is to analyze neuroimaging data to measure specific pathologies related to AD.

NEUROIMAGING AND ALZHEIMER'S DISEASE (AD)



PiB PET imaging

(Pittsburgh compound B) (Positron-emission tomography)

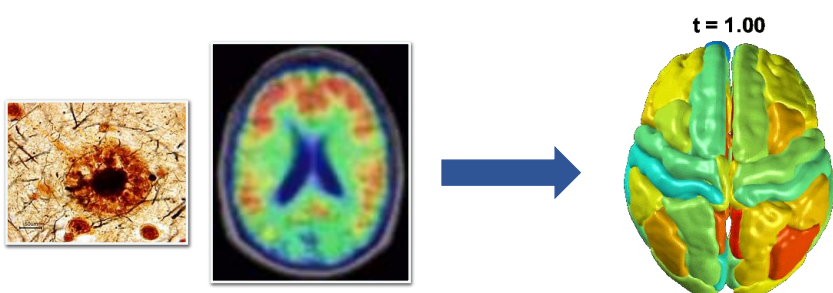
↑ PiB Distribution Volume Ratio \Rightarrow ↑Amyloid \Rightarrow ↑Risk of Dementia



For instance, PiB PET imaging specifically measures the amount of amyloid, by measuring the distribution volume ratio, OR DVR, of Pittsburgh compound B a PET radiotracer that binds to beta amyloid plaque in the brain. And Amyloid accumulation during time is acknowledged to be a primary pathological event in AD such that high amount of amyloid in the

brain is associated with high risk of dementia. When we look at this neuroimaging while time factor is involved, the PET imaging measures become longitudinal or sequential.

NEUROIMAGING AND ALZHEIMER'S DISEASE (AD)



PiB PET imaging

(Pittsburgh compound B) (Positron-emission tomography)

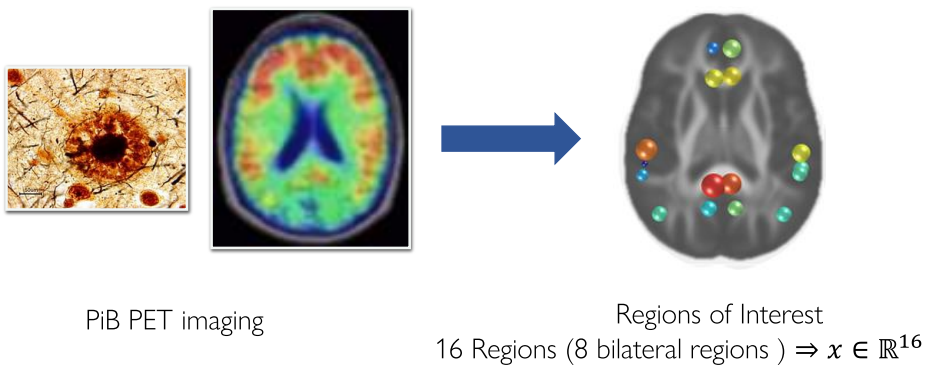
↑ PiB Distribution Volume Ratio \Rightarrow ↑Amyloid \Rightarrow ↑Risk of Dementia



For instance, PiB PET imaging specifically measures the amount of amyloid, by measuring the distribution volume ratio, OR DVR, of Pittsburgh compound B a PET radiotracer that binds to beta amyloid plaque in the brain. And Amyloid accumulation during time is acknowledged to be a primary pathological event in AD such that high amount of amyloid in the

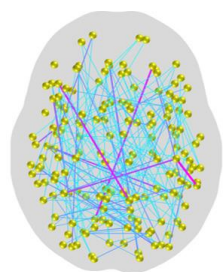
brain is associated with high risk of dementia. When we look at this neuroimaging while time factor is involved, the PET imaging measures become longitudinal or sequential.

NEUROIMAGING AND ALZHEIMER'S DISEASE (AD)



We sometimes focus on a subset of regions of interest in neuroimaging. In this figure, 16 gray matter regions known to be affected by AD are denoted using spheres for demonstration purpose.

NEUROIMAGING AND ALZHEIMER'S DISEASE (AD)



T1 Weighted Magnetic Resonance Imaging
MRI

Structural Brain Connectivity



Besides PET imaging, Magnetic resonance imaging is another important kind of neuroimaging. MRI measures spin-lattice relaxation during MRI scan which can inform the structural brain connectivity.

NEUROIMAGING AND ALZHEIMER'S DISEASE (AD)

Prion-like Transmission of AD Pathology along Structural Connectivity

Nat Rev Neurosci. 2010 Mar;11(3):155-9. doi: 10.1038/nrn2786. Epub 2009 Dec 23.
Prion-like mechanisms in neurodegenerative diseases.
Frost BJ¹, Diamond MI.

Nature. 2006 Oct 19;443(7113):768-73.
A network dysfunction perspective on neurodegenerative diseases.
Palop JJ¹, Chin J, Mucke L.

Acta Neuropathol. 2018; 136(1): 41–56.
Published online 2018 Jun 13. doi: 10.1007/s00401-018-1868-1
PMCID: PMC6015111
PMID: 29934873

Alzheimer's disease pathology propagation by exosomes containing toxic amyloid-beta oligomers
Maltrayes Sardar Simha,^{#1} Anna Ansart-Schultz,^{#1} Livia Civitelli,¹ Camilla Hildebrand,¹ Max Larsson,¹ Lars Lannfelt,^{2,3} Martin Ingelsson,² and Martin Hallbeck^{#1}

Nat Cell Biol. 2009 Jul;11(7):909-13. doi: 10.1038/ncb1901. Epub 2009 Jun 7.
Transmission and spreading of tauopathy in transgenic mouse brain.
Clavaguera F¹, Bolmont T, Croyther RA, Abramowski D, Frank S, Probst A, Fraser G, Stalder AK, Beibel M, Staufenbiel M, Jucker M, Goedert M, Tolnay M.

Acta Neuropathol. 2015 Sep;130(3):349-62. doi: 10.1007/s00401-015-1458-4.
Epub 2015 Jul 7.

Tau pathology spread in PS19 tau transgenic mice following locus coeruleus (LC) injections of synthetic tau fibrils is determined by the LC's afferent and efferent connections.
Iba M¹, McBride JD, Guo JL, Zhang B, Trojanowski JQ, Lee VM.

Nature. 2013 Sep 5;501(7465):45-51. doi: 10.1038/nature12481.
Self-propagation of pathogenic protein aggregates in neurodegenerative diseases.
Jucker M¹, Walker LC.

Prion-like propagation of β-amyloid aggregates in the absence of APP overexpression.
Ruiz-Riquelme A¹ , Lau HH¹, Stuart E¹, Goczi AN¹, Wang Z¹, Schmitt-Umlauf G¹, Watts JC¹ 
Author information 

Acta Neuropathologica Communications. 03 Apr 2018; 6(1):26
DOI: 10.1186/s40478-018-0529-x PMID: 29615128 PMCID: PMC5883524

This also helps us understand the amyloid accumulation. As more and more literatures suggest that propagation of amyloid is a prion-like transmission which occurs along neural pathways as a function of the disease process.

NEUROIMAGING AND ALZHEIMER'S DISEASE (AD)

Pattern of spread in the preclinical stages of AD ?

Nat Rev Neurosci. 2010 Mar;11(3):155-9. doi: 10.1038/nrn2786. Epub 2009 Dec 23.
Prion-like mechanisms in neurodegenerative diseases.
Frost B¹, Diamond MI.

Nature. 2006 Oct 19;443(7113):768-73.
A network dysfunction perspective on neurodegenerative diseases.
Palop JJ¹, Chin J, Mucke L.

Acta Neuropathol. 2018; 136(1): 41–56.
Published online 2018 Jun 13. doi: 10.1007/s00401-018-1868-1
PMCID: PMC6015111
PMID: 29934873

Alzheimer's disease pathology propagation by exosomes containing toxic amyloid-beta oligomers
Maltrayee Sardar Sima,^{#1} Anna Ansell-Schultz,^{#1} Livia Civitelli,¹ Camilla Hildesjö,¹ Max Larsson,¹ Lars Lannfelt,^{2,3} Martin Ingelsson,² and Martin Hallbeck^{#1}

Nat Cell Biol. 2009 Jul;11(7):909-13. doi: 10.1038/ncb1901. Epub 2009 Jun 7.
Transmission and spreading of tauopathy in transgenic mouse brain.
Clavaguera F¹, Bolmont T, Croyther RA, Abramowski D, Frank S, Probst A, Fraser G, Stalder AK, Beibel M, Staufenbiel M, Jucker M, Goedert M, Tolnay M.

Acta Neuropathol. 2015 Sep;130(3):349-62. doi: 10.1007/s00401-015-1458-4.
Epub 2015 Jul 7.

Tau pathology spread in PS19 tau transgenic mice following locus coeruleus (LC) injections of synthetic tau fibrils is determined by the LC's afferent and efferent connections.
Iba M¹, McBride JD, Guo JL, Zhang B, Trojanowski JQ, Lee VM,

Nature. 2013 Sep 5;501(7465):45-51. doi: 10.1038/nature12481.
Self-propagation of pathogenic protein aggregates in neurodegenerative diseases.
Jucker M¹, Walker LC.

Prion-like propagation of β-amyloid aggregates in the absence of APP overexpression.
Ruiz-Riquelme A¹ , Lau HH¹, Stuart E¹, Gocai AN¹, Wang Z¹, Schmitt-Ulms G¹, Watts J¹ 
Author information 

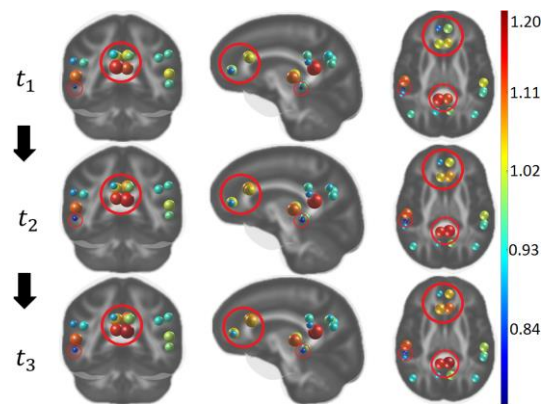
Acta Neuropathologica Communications. 03 Apr 2018; 6(1):26
DOI: 10.1186/s40478-018-0529-x PMID: 29615128 PMCID: PMC5883524

Though the two types of neuroimaging will help us along our way understanding AD, the pattern of spread in the preclinical stages of AD is still poorly understood. And Our work is motivated by this question.

PROBLEM SETUP

Goal: Predict individual-level amyloid burden at future time points in preclinical Alzheimer's disease (AD) using baseline image scans.

Importance: Predicting progression of AD pathology will facilitate identifying individuals most likely to benefit from anti-amyloid therapy.

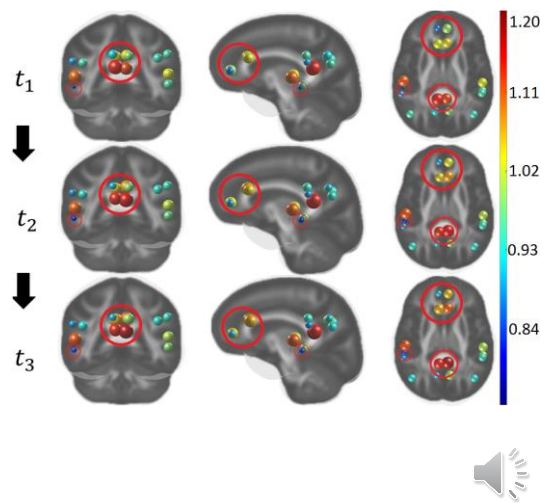


We try to predict individual-level amyloid burden at future time points in preclinical Alzheimer's disease (AD) using baseline neuroimaging scans. This is very meaningful because predicting progression of the pathology will facilitate identifying individuals who are most likely to benefit from anti-amyloid therapy.

PROBLEM SETUP

Goal: Predict individual-level amyloid burden at future time points in preclinical Alzheimer's disease (AD) using baseline image scans.

Challenge: Lack of methods for characterizing individual-level amyloid propagation patterns using both the individual amyloid scan as well as structural brain connectivity.



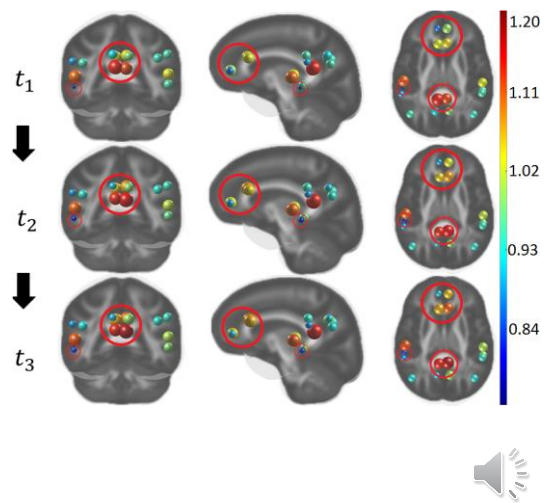
The challenge we face is the lack of methods for characterizing individual-level amyloid propagation patterns, using both the individual amyloid scan as well as structural brain connectivity. As mentioned before, the latter factor is important because the structural brain connectivity informs the fiber pathways which guide amyloid progression from one region to the other in

the brain.

PROBLEM SETUP

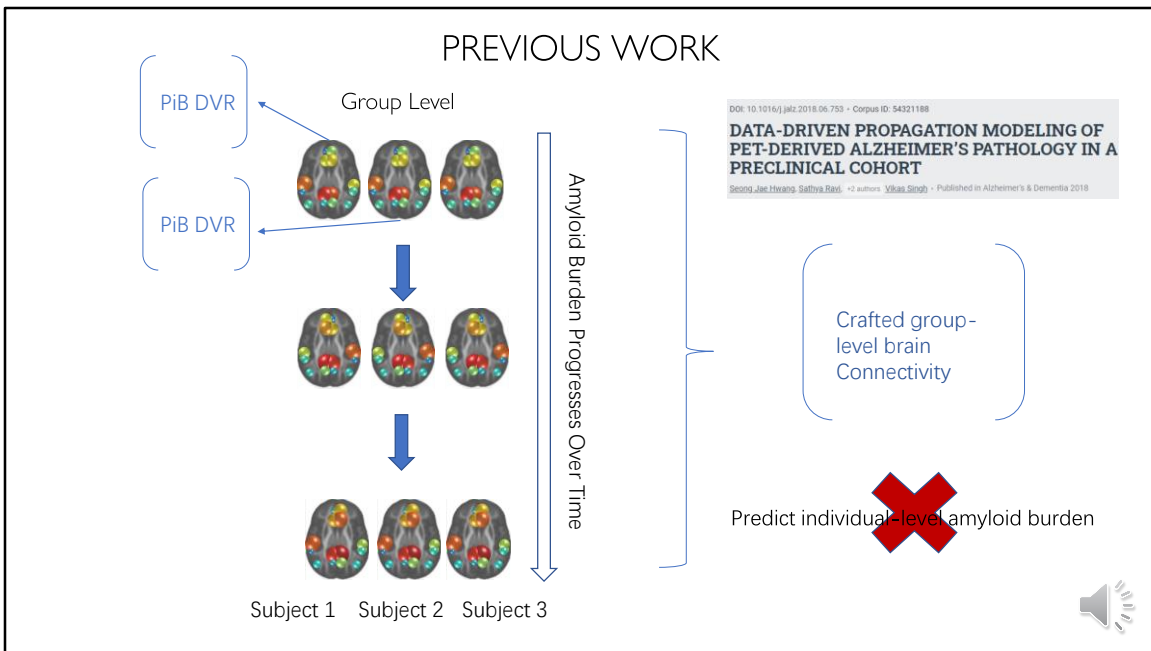
Goal: Predict individual-level amyloid burden at future time points in preclinical Alzheimer's disease (AD) using baseline image scans.

Challenge: Lack of methods for characterizing individual-level amyloid propagation patterns using both the individual amyloid scan as well as structural brain connectivity.



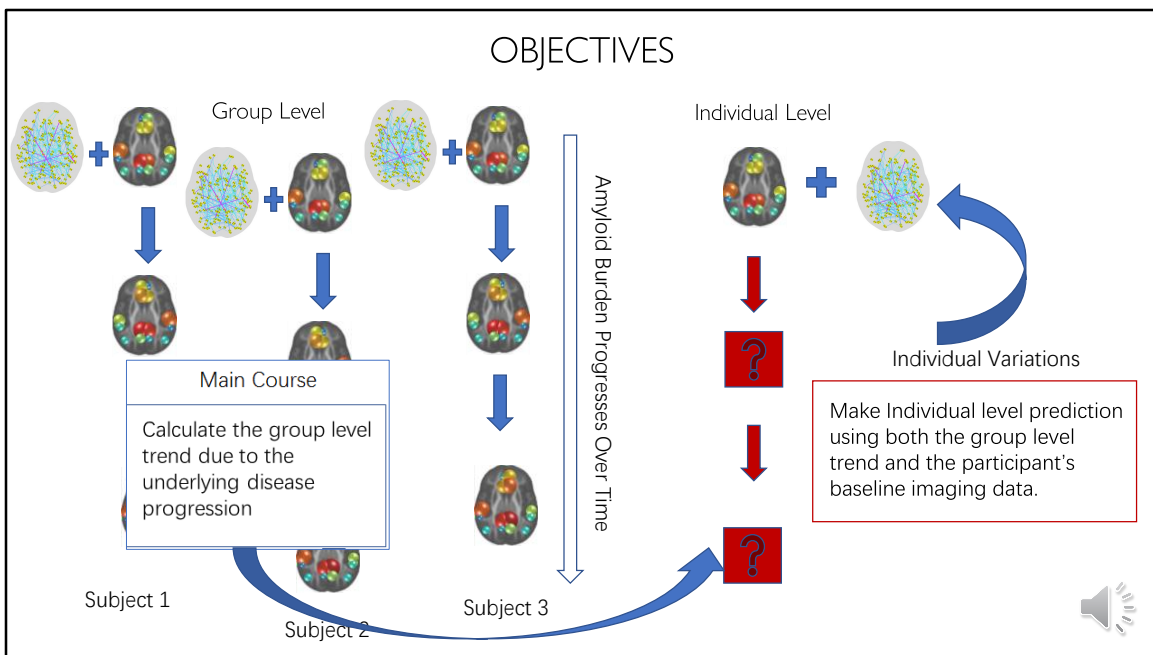
The challenge we face is the lack of methods for characterizing individual-level amyloid propagation patterns, using both the individual amyloid scan as well as structural brain connectivity. As mentioned before, the latter factor is important because the structural brain connectivity informs the fiber pathways which guide amyloid progression from one region to the other in

the brain.



In fact, instead of individual-level prediction, a previous work tried to capture the group-level amyloid propagation, based on the full cohort's amyloid scans. Its model infers a crafted group-level brain connectivity only from the PiB DVRs over time. However, this crafted group-level connectivity cannot be used to characterize the individual level propagation because the

derived propagation routes are for the full group and do not consider individual variations.



So, to characterize individual-level amyloid progression, we need to have a model, that knows how to map baseline PiB measurements to measurements over time, appropriately informed by the individual's connectivity information. This prior knowledge will act as the main course of group-level progression trend due to the underlying disease pattern. And the model

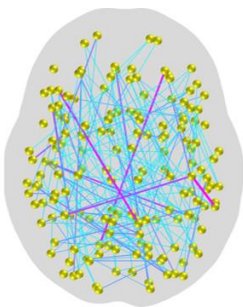
may use this knowledge to make individualized prediction.

1. NETWORK DIFFUSION MODEL



To begin describing our model, we start with the idea of network diffusion model.

NETWORK DIFFUSION MODEL



$$G_s = \{V ; E\} \quad \text{Region } i \in V ; \text{ Edge } i, j \in E$$

PiB DVR for the graph s at time t : $\phi(t)_s \in R^{\# \text{ of } V}$

$$\frac{d\phi(t)_s}{dt} = -k \cdot L_s \cdot \phi(t)_s$$

Diffusion Constant

Graph Laplacian



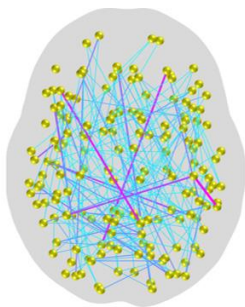
Let's imagine the brain as a connected graph s where brain regions are represented by vertices. And an edge means the existence of fiber path in between two regions.

Then, the amount of PiB DVR for the graph s at time t can be expressed by a vector $\Phi(t)_s$. When time passes, we can imagine the amyloid propagation as a heat diffusion process. And it can be written using a

differential equation as shown below. The constant k denotes the diffusion speed and L is the graph Laplacian which stores the brain connectivity information in a matrix format.

NETWORK DIFFUSION MODEL

$$\frac{d\phi(t)_s}{dt} = -k \cdot L_s \cdot \phi(t)_s$$

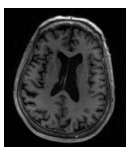


$$L(i,j)_s = \begin{cases} -c_{i,j} & \text{If } i \neq j \\ \sum_{(i,j') ; e_{i,j'} \in E} c_{i,j'} & \text{otherwise} \end{cases}$$

$c_{i,j}$ is the connectivity strength between region i and j. 

To be specific, each element in L can be expressed as shown. Where $c_{i,j}$ is the connectivity strength between region i and j. Noticeably, the graph Laplacian is symmetric.

NETWORK DIFFUSION MODEL

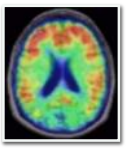


T1 Weighted MRI
Structural Brain Connectivity



Subject Level
Laplacian L_s
 16×16

Processed using the
Computational Anatomy
Toolbox and 'Graynet'



PiB PET Imaging
Detecting Amyloid Load



Subject Level
PiB DVR $\phi(t)_s$
 16×1



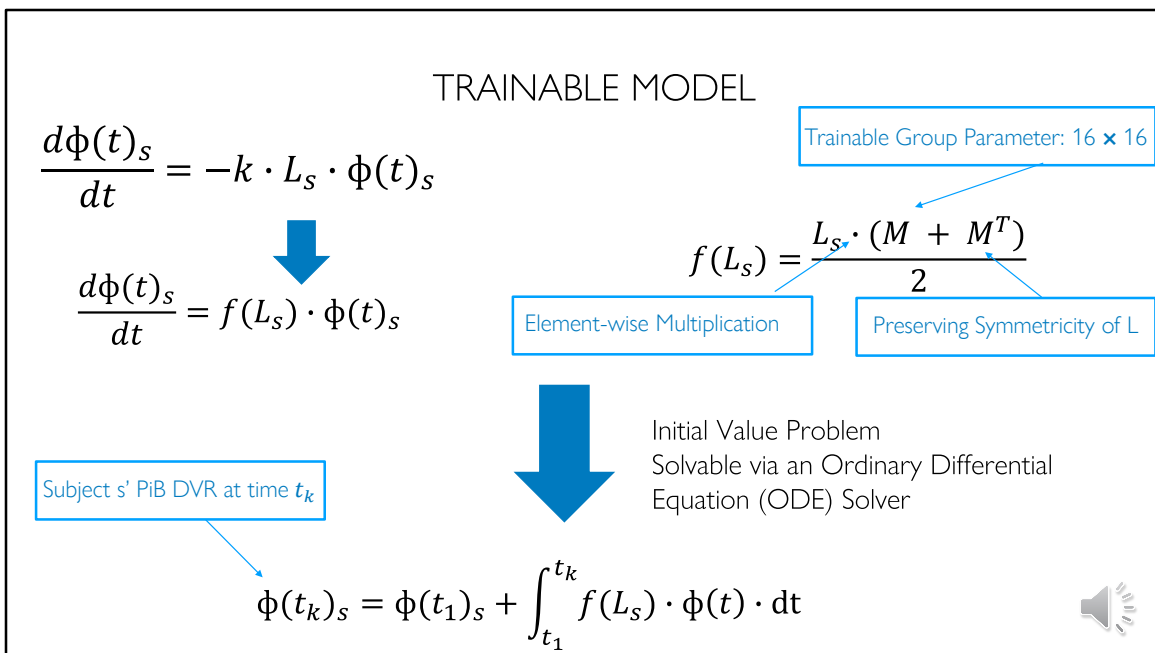
The connectivity strength can be derived from T1 Weighted MRI using the Computational Anatomy Toolbox and 'Graynet' which are referenced in our paper. Since we will focus on the 16 gray matter regions known to be affected by AD during the amyloid propagation, the graph Laplacian for a subject s can be expressed as a 16 by 16 matrix.

Correspondingly, the Phi for that subject can be expressed as a 16 by 1 vector. With

these information, we can start to formulate our model.

2. TRAINABLE MODEL

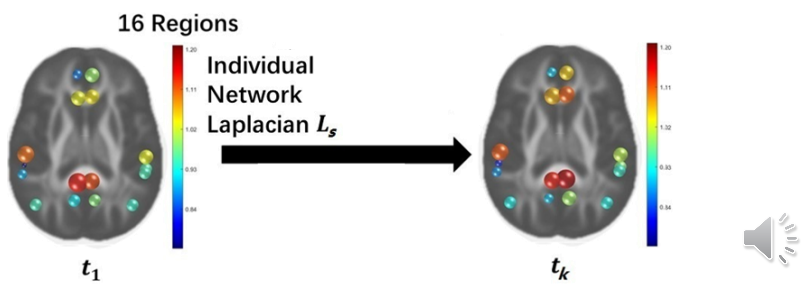




To let the brain structural connectivity inform the model, we need to find a function mapping an individual L as input to an $f(L)$ with the group trend applied. We construct the function f as the following format where the M will act as a to-be-learned group parameter. It has the same size as the input Laplacian. The M will store information about the cohort propagation.

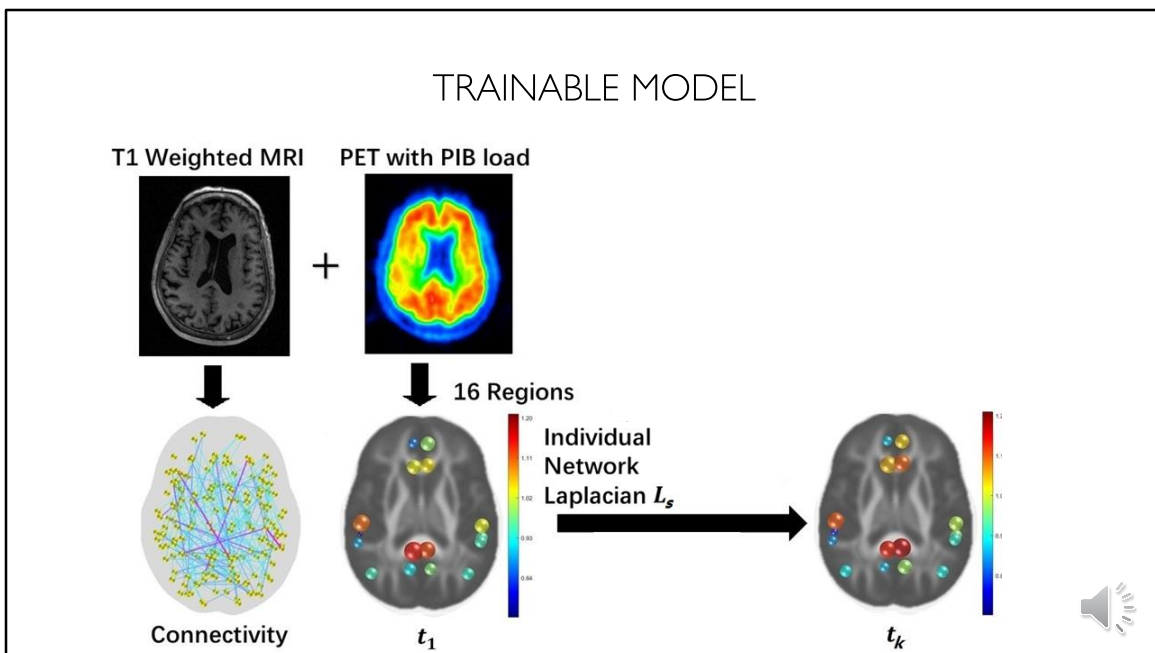
course and the function can add ‘individual variation’ to the ‘Main course’ by tuning M during the training process. In this format, predicting a subject’s PiB DVR at a future time point tk is formulated as an initial value problem. The problem is solvable via an ordinary differential equation solver which is referenced in our paper.

TRAINABLE MODEL



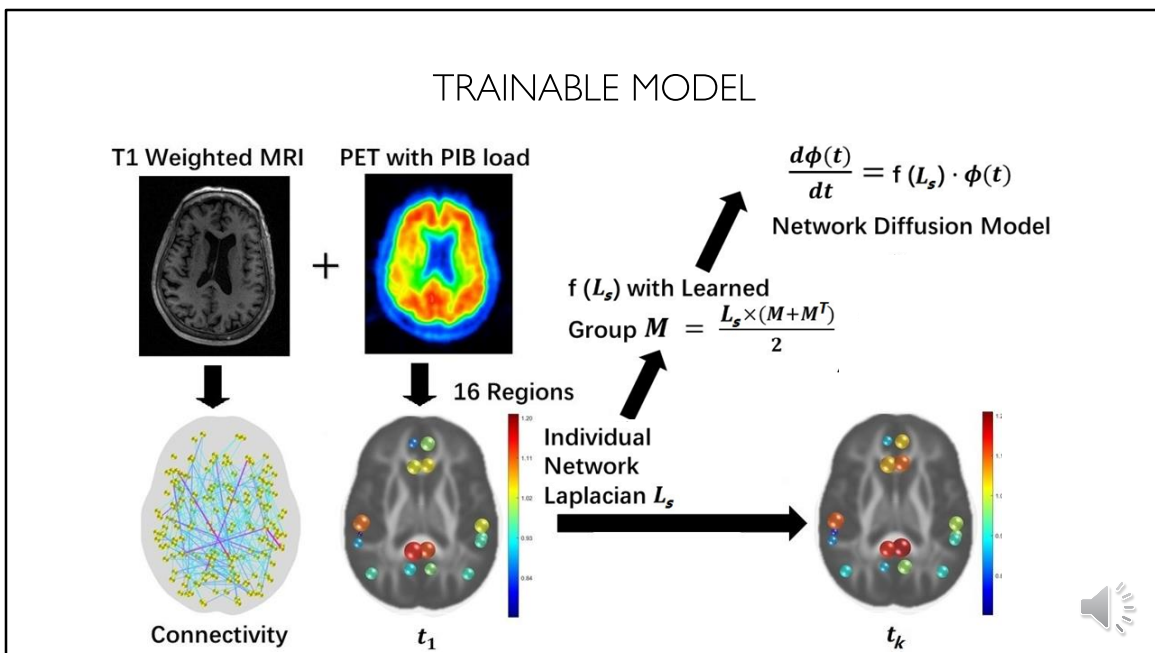
Here is a summary of our model. To predict a subject's PiB DVR at a future time point, the model takes the subject's structural brain connectivity expressed as a Laplacian and a vector of the initial PiB DVR as inputs. A learned group parameter is applied to the Laplacian and an initial value problem is established via the network diffusion model. The predicted PiB DVR is then calculated by

an ODE solver.



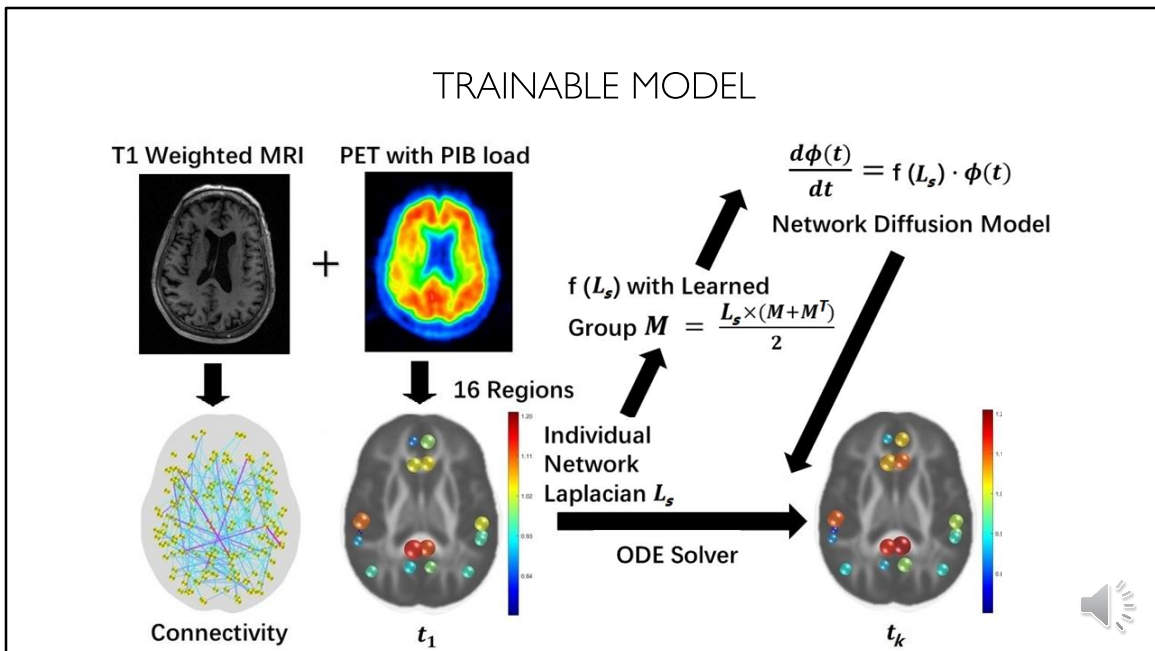
Here is a summary of our model. To predict a subject's PiB DVR at a future time point, the model takes the subject's structural brain connectivity expressed as a Laplacian and a vector of the initial PiB DVR as inputs. A learned group parameter is applied to the Laplacian and an initial value problem is established via the network diffusion model. The predicted PiB DVR is then calculated by

an ODE solver.



Here is a summary of our model. To predict a subject's PiB DVR at a future time point, the model takes the subject's structural brain connectivity expressed as a Laplacian and a vector of the initial PiB DVR as inputs. A learned group parameter is applied to the Laplacian and an initial value problem is established via the network diffusion model. The predicted PiB DVR is then calculated by

an ODE solver.



Here is a summary of our model. To predict a subject's PiB DVR at a future time point, the model takes the subject's structural brain connectivity expressed as a Laplacian and a vector of the initial PiB DVR as inputs. A learned group parameter is applied to the Laplacian and an initial value problem is established via the network diffusion model. The predicted PiB DVR is then calculated by

an ODE solver.

3. EXPERIMENTAL SETUP AND RESULTS



With the established model, we run some experiments to evaluate it on real data set.

EXPERIMENTAL SETUP

Dataset: Cognitively unimpaired subjects from Wisconsin Registry for Alzheimer's Prevention study.

N = 112, Baseline age: 67.6 ± 6 , % female: 68.6

Each subject s has:

1. $L_s \in R^{16 \times 16}$ from T1-weighted Imaging
2. $\phi(t_1)_s, \phi(t_2)_s, \phi(t_3)_s \in R^{16}$ from 3 time point PiB PET imaging



The longitudinal dataset is from Wisconsin Registry for Alzheimer's Prevention study. 112 cognitively unimpaired subjects with at least three time points of PiB-PET scans and baseline T1-weighted MRI were included.

MODEL EVALUATION

Two settings with different dataset splits:

1. Goal: Use baseline of held-out subjects to predict their $\phi(t_2)$

Training data: $\phi(t_1), \phi(t_2), L$

Number of training subjects: 90%

Prediction: predict $\phi(t_2)$ of remaining 10% (10-Cross Validation)

2. Goal: Use baselines of trained subjects to predict their $\phi(t_3)$

Train data: $\phi(t_1), \phi(t_2), L$

Number of training subjects: All

Prediction: predict $\phi(t_3)$ of all subjects



We evaluate the model in two settings with different dataset splits. The training data in the first setting includes 90% of the subjects and the Model is trained using $\phi(t_1), \phi(t_2)$ and L . We estimate the accuracy of estimated amyloid loads at t_2 given only the baseline $\phi(t_1)$ on the remaining 10% subjects. And we perform a 10-fold cross-validation.

The training data in the second setting includes all of the subjects and the Model is trained using $\Phi(t_1), \Phi(t_2)$ and L where scans at t_3 are held out. We estimate the accuracy of estimated amyloid loads at t_3 given only the baseline $\Phi(t_1)$ on all subjects.

COMPARISON WITH INFERENCE BASED ON LINEAR ESTIMATE

$$\widehat{\phi}'(t_k)_s = \phi(t_1)_s + \frac{\sum_{s'=1, s' \neq s}^n (\phi(t_k)_{s'} - \phi(t_1)_{s'})}{n-1}$$

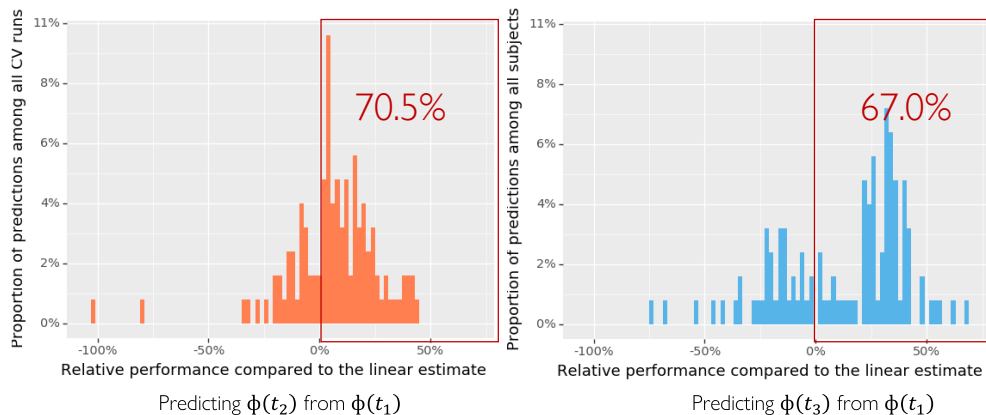
↑ ↑
Baseline PiB DVR Linear Estimate



We compare our prediction ϕ' with a simple prediction made by a naïve linear estimate method denoted using $\widehat{\phi}'$.

COMPARISON WITH INFERENCE BASED ON LINEAR ESTIMATE

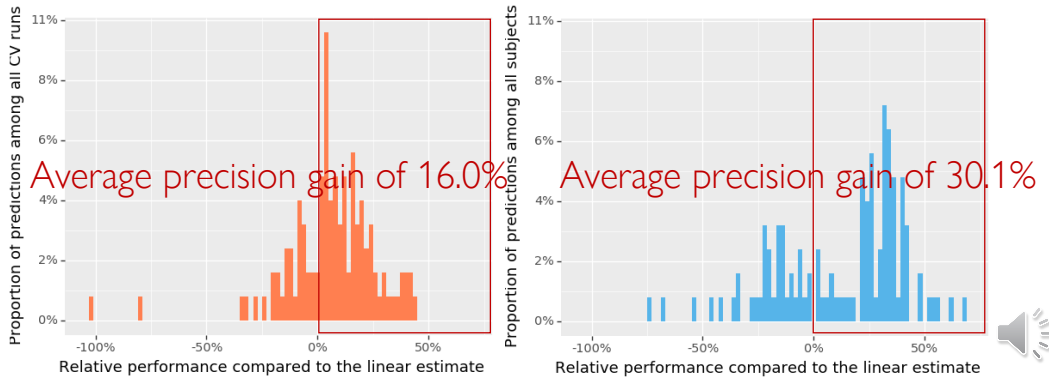
$$\widehat{\phi}'(t_k)_s = \phi(t_1)_s + \frac{\sum_{s'=1, s' \neq s}^n (\phi(t_k)_{s'} - \phi(t_1)_{s'})}{n-1}$$



The figure below shows that our model yields more accurate predictions of PiB-PET measurements in 70.5% of t2 samples and 67.0% of t3 samples, compared with the linear estimate.

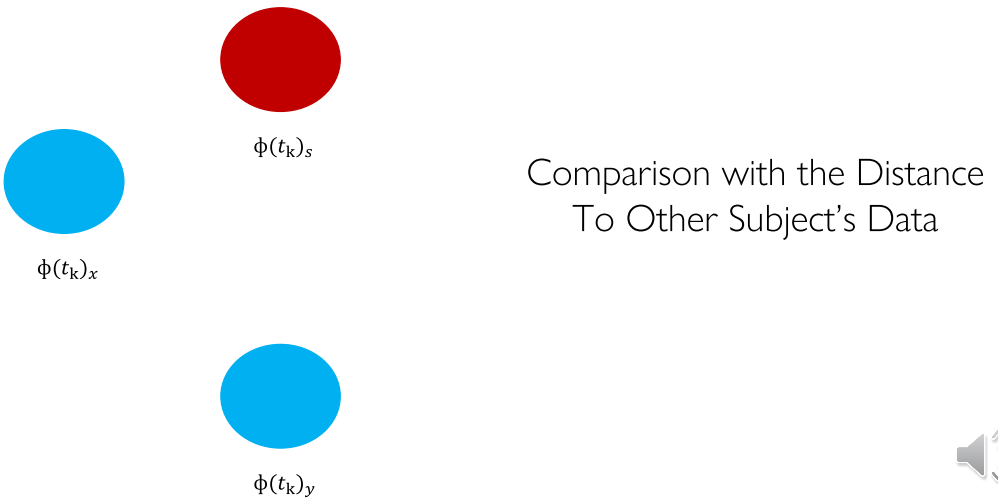
COMPARISON WITH INFERENCE BASED ON LINEAR ESTIMATE

$$\frac{1}{n} \sum_{s=1}^n \frac{\|\phi(t_k)_s - \widehat{\phi}'(t_k)_s\|_2 - \|\phi(t_k)_s - \widehat{\phi}(t_k)_s\|_2}{\|\phi(t_k)_s - \widehat{\phi}'(t_k)_s\|_2}$$



We also calculated how good our predictions are when they outperform the linear estimates. The figure and numbers tell us that our model captures most of the propagation patterns and performs better at a further time point t3 when only the baseline scans of each subject is available

HOW CLOSE IS OUR PREDICTION TO THE REAL DATA?



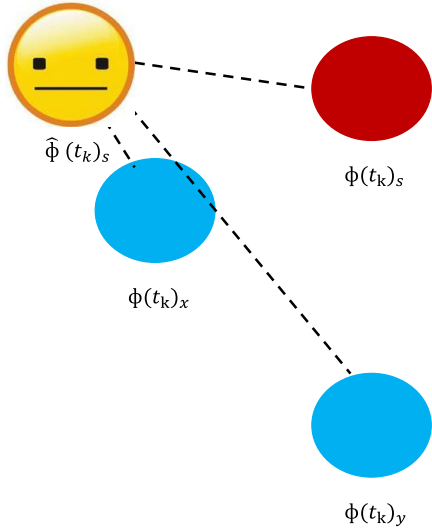
Another question we ask when performing evaluation is: how close is our prediction to the real data? We ask this question in two analogous scenarios:

First,

Among all test subjects, the L2-norm is calculated between our prediction $\hat{\Phi}(t_k)_s$ for subject s and real DVR vector $\Phi(t_k)$ for each test subject. The most ideal case is that

our prediction is the closest towards the subject s' $\phi(t_k)_s$ other than other test subject's $\phi(t_k)$, since we are performing the prediction for that particular subject s, not for other subjects. So, the closer our prediction towards the real DVR data we are targeting, the better the model is.

HOW CLOSE IS OUR PREDICTION TO THE REAL DATA?



Comparison with the Distance
To Other Subject's Data



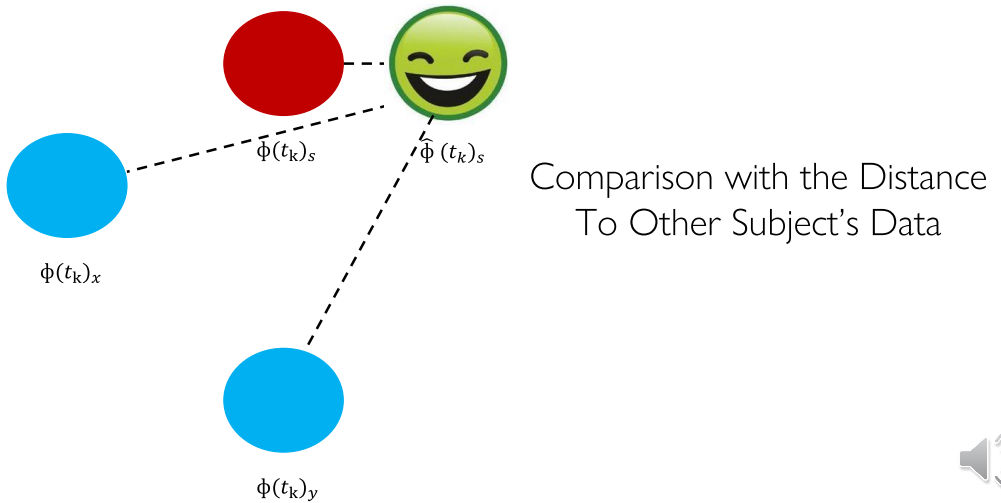
Another question we ask when performing evaluation is: how close is our prediction to the real data? We ask this question in two analogous scenarios:

First,

Among all test subjects, the L2-norm is calculated between our prediction $\hat{\Phi}(t_k)_s$ for subject s and real DVR vector $\Phi(t_k)$ for each test subject. The most ideal case is that

our prediction is the closest towards the subject s' $\phi(t_k)_s$ other than other test subject's $\phi(t_k)$, since we are performing the prediction for that particular subject s, not for other subjects. So, the closer our prediction towards the real DVR data we are targeting, the better the model is.

HOW CLOSE IS OUR PREDICTION TO THE REAL DATA?



Another question we ask when performing evaluation is: how close is our prediction to the real data? We ask this question in two analogous scenarios:

First,

Among all test subjects, the L2-norm is calculated between our prediction $\hat{\Phi}(t_k)_s$ for subject s and real DVR vector $\phi(t_k)$ for each test subject. The most ideal case is that

our prediction is the closest towards the subject s' $\phi(t_k)_s$ other than other test subject's $\phi(t_k)$, since we are performing the prediction for that particular subject s, not for other subjects. So, the closer our prediction towards the real DVR data we are targeting, the better the model is.

HOW CLOSE IS OUR PREDICTION TO THE REAL DATA?



$\phi(t_k)_s$



Randomly Generated data



$\hat{\phi}(t_k)_s$



Randomly Generated data

Comparison with the Randomly Generated Data



The second scenario for the ‘how close question’ is: to compare our prediction with 99 randomly generated phi hat data that come from a certain distribution which artificially “simulate” test subjects. Similarly, the less artificial test subjects in between our prediction towards the real DVR data of subject s, the better the model is.

HOW CLOSE IS OUR PREDICTION TO THE REAL DATA?



$\phi(t_k)_s$



$\hat{\phi}(t_k)_s$



Randomly Generated data



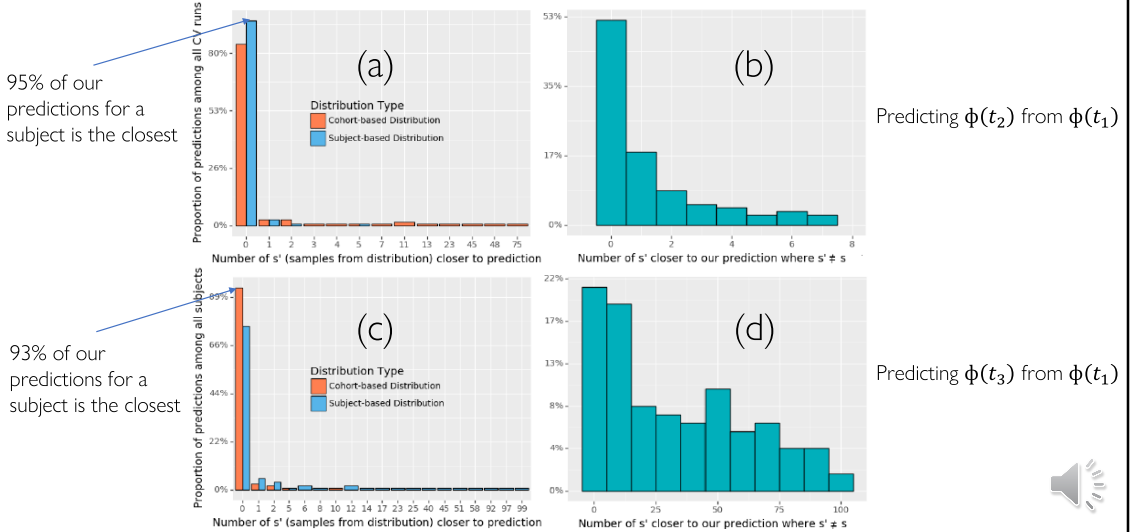
Randomly Generated data

Comparison with the Randomly Generated Data



The second scenario for the ‘how close question’ is: to compare our prediction with 99 randomly generated phi hat data that come from a certain distribution which artificially “simulate” test subjects. Similarly, the less artificial test subjects in between our prediction towards the real DVR data of subject s, the better the model is.

HOW CLOSE IS OUR PREDICTION TO THE REAL DATA?

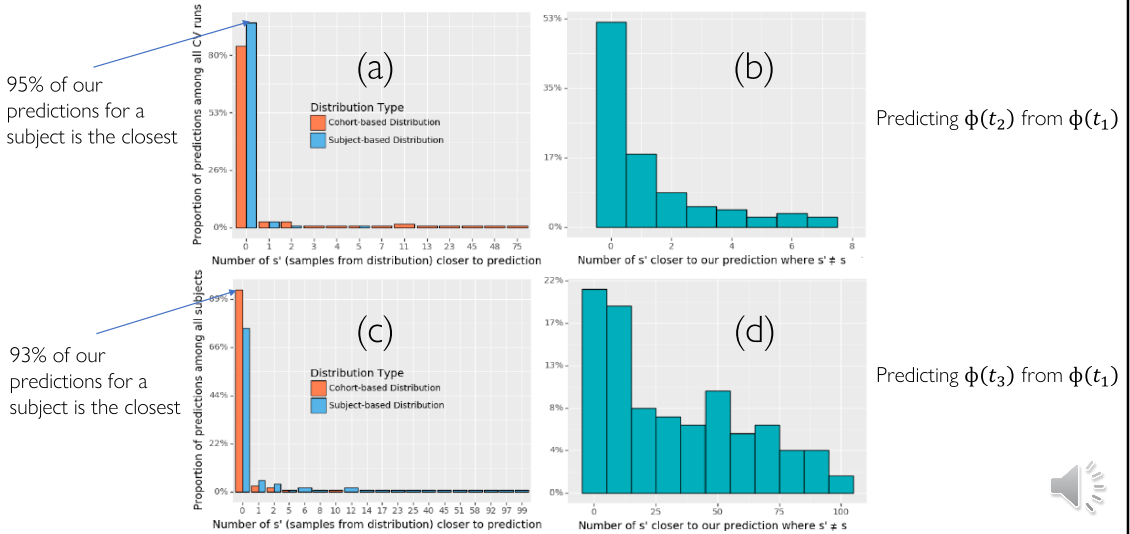


Let's look at the result. In Figure (a) and (c), we use the cohort distribution and the individual's measurement distribution to artificially "simulate" test subjects for predicting $\phi(t_2)$ and $\phi(t_3)$ in our second scenario. The detailed method for generating random data are described in our paper. In both cases, we find that the model performs well. 95% and 93% of our predictions for a



subject is the closest towards the real DVR data for predicting ϕ t2 and ϕ t3 respectively. Similarly, Figure (b) and (d) show reasonably good results for measuring the “how close” question regards to our first scenario when we do comparison with the distance to other Subject’s Data.

HOW CLOSE IS OUR PREDICTION TO THE REAL DATA?



Let's look at the result. In Figure (a) and (c), we use the cohort distribution and the individual's measurement distribution to artificially "simulate" test subjects for predicting $\phi(t_2)$ and $\phi(t_3)$ in our second scenario. The detailed method for generating random data are described in our paper. In both cases, we find that the model performs well. 95% and 93% of our predictions for a

subject is the closest towards the real DVR data for predicting ϕ t2 and ϕ t3 respectively. Similarly, Figure (b) and (d) show reasonably good results for measuring the “how close” question regards to our first scenario when we do comparison with the distance to other Subject’s Data.

GROUP DIFFERENCE ANALYSIS: APOE e4 + vs. APOE e4 -

- APOE e4:

The APOE gene provides instructions for making a protein called apolipoprotein E & one allele, APOE e4 is associated with Alzheimer's disease since it's a risk factor for beta protein deposition.



The last question we want to ask for evaluation is: can our model find the different amyloid progression pattern between two distinct groups?

So, we choose to do a group difference analysis via statistical test between the apo e4+ and the apo e4- group where APOE e4 is the risk genotype for Alzheimer's disease.

GROUP DIFFERENCE ANALYSIS: APOE e4 + vs. APOE e4 -

- APOE e4:

The APOE gene provides instructions for making a protein called apolipoprotein E & one allele, APOE e4 is associated with Alzheimer's disease since its a risk factor for beta protein deposition.

Statistical Test

- Split the dataset and train two models : APOE e4 + (n = 45) and APOE e4 - (n = 67).
- l_2 norm between M_1 and M_2 (the learned group parameters) from two models is computed ---the statistical summary for the correct group.
- **Null Hypothesis H_0** : There is no group level difference between the parameters within these two groups.



To setup, we split the dataset with an APOE e4 positive group of 45 subjects and an APOE e4 negative group of 67 subjects. We then train two models based on the split. we computed the l_2 norm between M_1 and M_2 from the two models as the statistical summary for the correct group.

Our Null Hypothesis *is* that There is no group level difference between the

parameters within these two groups.

GROUP DIFFERENCE ANALYSIS: APOE e4 + vs. APOE e4 -

Permutation Testing:

1. split data randomly with same group sizes (45 and 67)
2. Calculate the difference between M_s from the two models
3. Repeat for 10K draws
4. Derive null distribution of summary statistic
5. Compute p-value



We then do a permutation Testing following the procedure below for 10K draws to derive null distribution of summary statistic and compute the p-value.

As a result, the p-value is way smaller than the significance threshold. This implies that our model captures the difference of amyloid progression pattern in the two groups. Which further implies the capture of

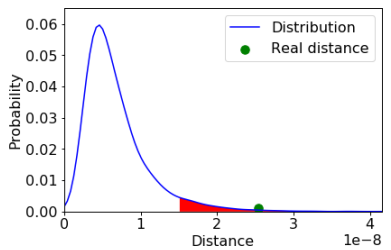
amyloid propagation dynamic in the pre-clinical stage of AD.

GROUP DIFFERENCE ANALYSIS: APOE e4 + vs. APOE e4 -

Permutation Testing:

1. split data randomly with same group sizes (45 and 67)
2. Calculate the difference between M_s from the two models
3. Repeat for 10K draws
4. Derive null distribution of summary statistic
5. Compute p-value

Result: The p-value is 0.00467 which is smaller than the significance threshold = 0.05.



Our model captures the difference of amyloid progression pattern in APOE e4 + and APOE e4 - groups



We then do a permutation Testing following the procedure below for 10K draws to derive null distribution of summary statistic and compute the p-value.

As a result, the p-value is way smaller than the significance threshold. This implies that our model captures the difference of amyloid progression pattern in the two groups. Which further implies the capture of

amyloid propagation dynamic in the pre-clinical stage of AD.

CONCLUSION & FUTURE WORK

1. Our model successfully predicts individual-level amyloid burden at future time points in preclinical Alzheimer's disease (AD) using both the individual amyloid scan as well as structural brain connectivity.



Lastly, I want to draw a conclusion that :Our model successfully predict individual-level amyloid burden at future time points in preclinical Alzheimer's disease (AD) using both the individual amyloid scan as well as structural brain connectivity.

For the future work:

Recent studies have shown that the early amyloid accumulation patterns may be a strong indicator of AD-related cognitive decline.

Our model could serve as a way to estimate the early amyloid accumulation trajectory in the unobserved past (e.g., $t < 1$) by “reversing” the direction of the prediction process (sign change of $f(L)$) and estimating the start time of amyloid accumulation.

CONCLUSION & FUTURE WORK

1. Our model successfully predicts individual-level amyloid burden at future time points in preclinical Alzheimer's disease (AD) using both the individual amyloid scan as well as structural brain connectivity.
2. Recent studies have shown that the early amyloid accumulation patterns may be a strong indicator of AD-related cognitive decline.

Our model could serve as a way to estimate the early amyloid accumulation trajectory in the unobserved past (e.g., $t < 1$) by “reversing” the direction of the prediction process (sign change of $f(L)$) and estimating the start time of amyloid accumulation.



Lastly, I want to draw a conclusion that :Our model successfully predict individual-level amyloid burden at future time points in preclinical Alzheimer's disease (AD) using both the individual amyloid scan as well as structural brain connectivity.

For the future work:

Recent studies have shown that the early amyloid accumulation patterns may be a strong indicator of AD-related cognitive decline.

Our model could serve as a way to estimate the early amyloid accumulation trajectory in the unobserved past (e.g., $t < 1$) by “reversing” the direction of the prediction process (sign change of $f(L)$) and estimating the start time of amyloid accumulation.

COLLABORATORS AND ACKNOWLEDGMENTS

Wei Hao Nicholas M. Vogt Zihang Meng Seong Jae Hwang Rebecca L. Koscik
Sterling C. Johnson Barbara B. Bendlin Vikas Singh

Acknowledgments. This project was supported in part by RF1 AG059312, R01 AG037639, R01 AG027161, R01 AG021155, P50 AG033514, UW CPCP (U54AI117924) and NSF CAREER award RI 1252725.



Github: <https://github.com/vsingh-group/ISBI>



Wisconsin Alzheimer's
Disease Research Center
UNIVERSITY OF WISCONSIN
SCHOOL OF MEDICINE AND PUBLIC HEALTH

Thank you very much for listening.